https://doi.org/10.22226/2410-3535-2023-2-138-142

Wear resistance of $Fe_{66}Cr_{10}Nb_5B_{19}$ detonation coatings under dry linearly reciprocating conditions and nanoscratch test

I. D. Kuchumova[†,1,2], V. S. Shikalov[3], I. S. Batraev[1], A. A. Filippov[3], G. Yu. Koga[4]

[†]ivannakz@mail.ru

[1]Lavrentyev Institute of Hydrodynamics SB RAS, Novosibirsk, 630090, Russia
[2]Novosibirsk State Technical University, Novosibirsk, 630073, Russia
[3]Khristianovich Institute of Theoretical and Applied Mechanics SB RAS, Novosibirsk, 630090, Russia
[4]Department of Materials Science and Engineering, Federal University of São Carlos, Via Washington Luiz, km 235, São Carlos, SP 13565-905, Brazil

The $Fe_{66}Cr_{10}Nb_5B_{19}$ alloy coatings with high hardness (≈850 HV_{300}), low porosity (less 3%), low content of crystalline phase (less 2.5 wt.%), elevated nanohardness (average value 13.7 GPa), and high wear resistance were obtained in a wide range of detonation spraying modes. The results of dry linearly reciprocating sliding wear tests of coatings carried out according to ASTM G 133-05 are presented. The wear resistance of coatings obtained at an explosive charge of 50 – 70% is significantly higher than that of stainless steel. The similar values of volume scratches of $Fe_{66}Cr_{10}Nb_5B_{19}$ coatings obtained at an explosive charge of 40 – 70% are attributed to the similar values of porosity and the content of the crystalline phase. Scratch and spalling are the main mechanisms of coatings destruction during scratching with a diamond tip.

Keywords: coating, glass structure, wear resistance, nanohardness, nanoscratch test.

1. Introduction

The fabrication of functional coatings by thermal spraying can improve the performance characteristics of the working surface, increase the reliability and lifespan of engineering components under wear and corrosion. Fe-based glassy alloys are promising materials for use as wear and corrosion resistant coatings obtained by thermal spraying technologies [1]. Fe-based bulk metallic glasses have shown high strength, high hardness, superior corrosion and wear resistance [2 – 4]. In the last few decades, interest has increased in the development of new compositions of amorphous alloys and the study of their properties [5, 6]. Fe-based glassy alloys are of interest because of their low cost related to iron, but at the same time exhibiting a high glass-forming ability [7]. The results of studying the tribological properties of thermal sprayed Fe-based glassy coatings are presented in [8 – 10]. It was shown that the content of the crystalline phase in the coatings, particularly boride nanocrystals, enhanced the hardness and wear resistance. As discussed in [11–14], reinforcement with harder particles and additional heat treatment can also be used to improve the wear resistance of coatings with a retained glassy structure. The corrosion resistance of glassy coatings is predominantly dependent on the content of the glassy phase and porosity [15].

Nanoscratch testing has now become a simple and versatile method for evaluating wear resistance and investigating the deformation of thin films, thick coatings, and bulk materials. Hodge and Nieh found that the wear resistance of the Zr-based and Pd-based glassy alloys when tested for nanoscratches did not obey the classical Archard's equation, i. e., the wear resistance was not linearly proportional to the hardness [16]. Glassy coatings also contain oxides, pores, and other heterogeneous phases that can lead to more complex behavior than bulk metallic glasses. During the spraying process, oxide films can form on the surface of the sprayed particles, and this can have a negative influence on the properties of the coatings [17 – 22]. Among the methods of thermal spraying, the impulse nature of detonation spraying allows the formation of wear resistant and dense coatings with a low content of the crystalline phase [23]. The results of a study of the tribological and corrosion properties of $Fe_{51.33}Cr_{14.9}Mo_{25.67}Y_{3.4}C_{3.44}B_{1.26}$ detonation coatings with a high content of the amorphous phase (content of crystalline phase 14.46 wt.%) was presented in [24]. Due to the formation of coatings with a partially crystalline structure and low porosity (less than 2%), the wear resistance was five-fold higher than that of stainless steel, which was used as the substrate material. However, there are few special studies in the literature on the processing window for ensuring the wear resistant Fe-based glassy coating produced by detonation spraying.

The present work was aimed to study the wear resistance under dry linearly reciprocating sliding wear and nanoscratching of $Fe_{66}Cr_{10}Nb_5B_{19}$ detonation coatings with an appreciable glassy structure obtained with different explosive charges (fractions of the barrel volume filled with an explosive mixture).

2. Materials and experimental methods

Detailed investigations of the phase composition and structure of the initial powder of the $Fe_{66}Cr_{10}Nb_5B_{19}$ alloy

with a particle size of 45 – 75 μm, which was used for detonation spraying in the present studies, were shown in our previous work [25]. The powder had a spherical shape and a high content of the glassy phase (≈69 wt.%). The glass transition temperature and crystallization temperature of the $Fe_{66}Cr_{10}Nb_5B_{19}$ alloy were determined as $T_g = 794$ K and $T_x = 846$ K, respectively. The alloy melts at $T_s = 1442$ K. This quaternary alloy shows a high glass-forming ability with a wide supercooled liquid region ($\Delta T = T_x - T_g$) equal to 52 K. For example, the alloys $Fe_{81}Si_{1.9}B_{5.7}P_{11.4}$ [26], $Fe_{67}Nb_4Si_5B_{14}$ [27] and $Fe_{48}Mo_{14}Cr_{15}Y_2C_{15}B_6$ [28] showed ΔT equal to 32°C, 45°C and 69°C, respectively; the latter containing considerable content of expensive alloying elements such as Mo and Y.

In our previous studies [17, 25], the detonation spraying modes of $Fe_{66}Cr_{10}Nb_5B_{19}$ powder with a particle size of 45 – 75 μm were determined. It was shown that using 50 – 60% of an explosive charge at a molar ratio O_2/C_2H_2 of 1.1 allowed to obtain high-quality dense coatings (thickness 200 – 350 μm) with high content of the glassy phase (less 2 wt.% of crystalline phase).

In the presented work, coatings with a thickness of 500 μm were obtained using 40 – 70% of explosive charge at a ratio O_2/C_2H_2 of 1.1, on the carbon steel substrate (grade St3, GOST 380 – 2005, analog to AISI A570). The substrates were cooled by compressed air during spraying. The content of the crystalline phase in the coatings obtained at 40%, 50%, 60%, and 70% of explosive charges was 2.5 , 2, 1.5, and 1 wt.%, respectively, as determined from the X-ray diffraction patterns by the Rietveld method using TOPAS 4.2 software (Bruker AXS). Bonding strength of $Fe_{66}Cr_{10}Nb_5B_{19}$ coatings measured by pin test method was 150 MPa [25].

The $Fe_{66}Cr_{10}Nb_5B_{19}$ detonation coatings with a glassy structure had a high resistance to atmospheric [29] and electrochemical corrosion [30]. Developed coatings can be recommended as protective coatings in aggressive environments. Due to the high corrosion resistance of $Fe_{66}Cr_{10}Nb_5B_{19}$ coatings, stainless steel (grade 12Cr18Ni10Ti, GOST 2590 – 2006, analog to AISI 321) was chosen as a reference material in this work.

The hardness of the coatings was measured using a semi-automatic Wolpert 402 MVD tester at a load of 300 g on the polished cross-sections of the coatings. A 136° pyramidal diamond indenter was used for measurements that forms a square indent. The average values of hardness were determined from 10 measurements. The effect of low electrical potentials on the microhardness, creep and microstructure of metallic materials has been studied in [31 – 33]. In present work hardness and scratch testings were made without electrical potentials. The standard wear tests of the $Fe_{66}Cr_{10}Nb_5B_{19}$ detonation coatings and stainless steel were performed according ASTM G 133 – 05 (Procedure A) using a ball-on-flat universal wear machine (UMT-2, Bruker). The diameter of a counterpart (WC-6Co ball) was 6.35 mm. The counterpart under applied load was sliding against the flat specimen of the samples (Fig. 1a). Before testing for wear, nanoscratch and nanoindentation tests the surface of the detonation coatings were ground, polished and degreased with acetone. The morphology of the worn surface after wear tests was studied by scanning electron microscopy (EVO50 XVP microscope, Carl Zeiss). The coefficient of friction (COF) was analyzed for reciprocating dry sliding tests. The wear resistance (R_w) of the coatings and stainless steel was calculated by the equation: $R_w = NS / V_w$, where N is the applied load, S and V_w are the total sliding distance and the worn volume, respectively [34]. The average values of wear resistance were calculated after 5 measurements.

Nanoindentation and nanoscratch tests were carried out using a Nanoscan 4D+ (TISNCM) scanning nanohardness tester with a standard three-sided pyramid Berkovich tip (an angle between the axis and a facet of 65° and tip radius 200 nm) on the polished surface. Areas on the coating surface without pores were selected for the measurements. For nanoindentation tests a normal load of 100 μN, a loading rate of 10 μN/s, and a peak load holding time of 2 s were applied.

Nanoscratch tests were conducted under rumping loads from 10 to 100 μN at a loading rate of 10 μN/s at a traverse speed of 0.5 μm/s over a scratch length of 100 μm (Fig. 1b). After the scratch test, the wear tracks were investigated by optical profilometry coupled to Vision64 software for calculation volume loss. The average values of nanohardness and nanoscratch were determined from 10 ×10 grid of indents (100 indents) and 5 measurements, respectively.

3. Results and discussion

3.1. Microstructure, hardness and wear resistance under dry linearly reciprocating sliding conditions of coatings

Figure 2 shows morphology and cross-sections of the detonation coating obtained at 70% of the explosive charge

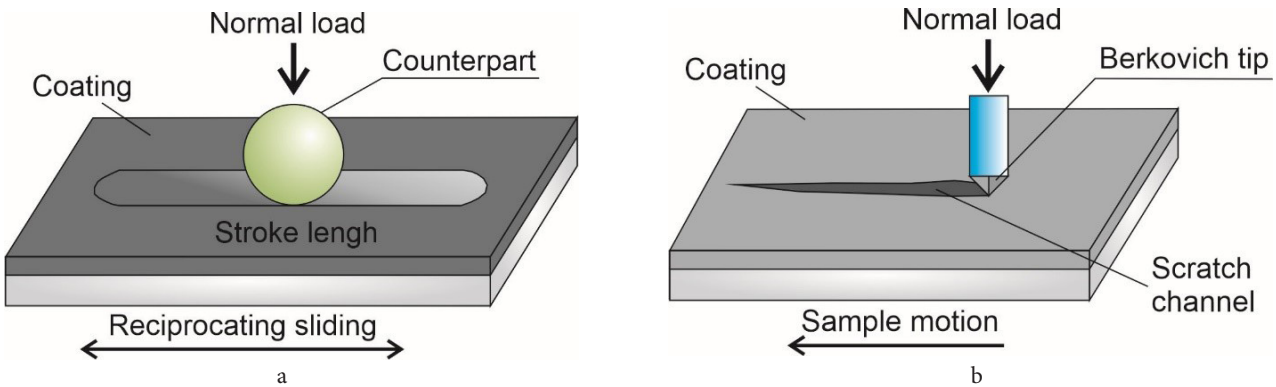

Fig. 1. The diagram of dry linearly reciprocating sliding test (a) and nanoscratch test (b).

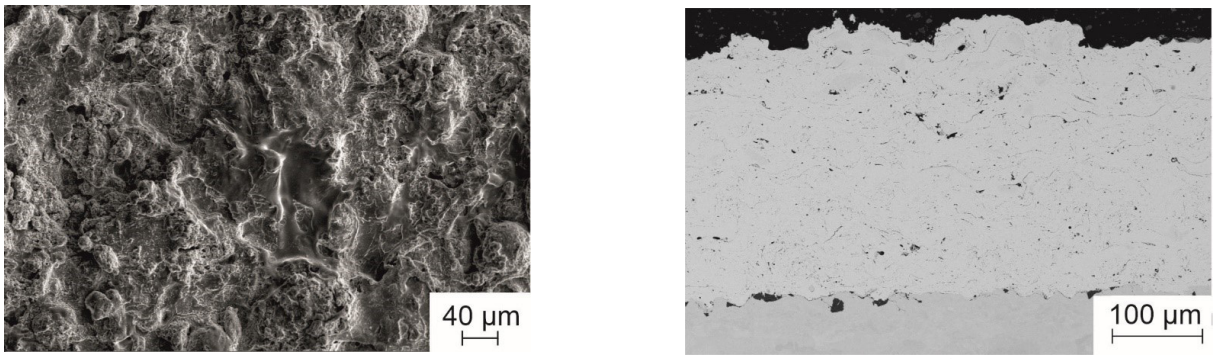

a b

Fig. 2. The morphology (a) and cross-sections (b) of the detonation coating obtained at 70% of the explosive charge.

(O_2/C_2H_2=1.1). The presented micrographs are typical for the obtained $Fe_{66}Cr_{10}Nb_5B_{19}$ coatings. Melted and unmelted particles can be seen on the coating surface (Fig. 2 a). The coatings possess a lamellar structure typical for thermal sprayed coatings (Fig. 2 b). Except for the coating obtained at 40% of an explosive charge, where the porosity was ≈3%, the porosity of other coatings was less than was less than 1%.

The results of $Fe_{66}Cr_{10}Nb_5B_{19}$ coatings microstructure investigations by transmission electron diffraction microscopy proved the amorphous structure of coatings [25]. Nanocrystals with chemical compositions corresponding to the initial alloy were found at the inter-splat boundaries. In the coating/substrate interface, alumina oxide particles can be present, which are artifacts after the sandblasting. The surface roughness after polishing was approximately R_a = 0.03 μm.

Results of measurements of Vickers hardness, average COF value in the steady-state stage, volume loss and wear resistance of $Fe_{66}Cr_{10}Nb_5B_{19}$ glassy coatings and stainless steel are presented in Table 1. The cross-sectional hardness of the detonation coatings obtained at 40%, 50%, 60%, and 70% of the explosive charge were 770, 870, 855, and 840 HV_{300}, respectively. The observed hardness of the glassy coatings (average value ≈850 HV_{300}) is close to the hardness of some Fe-based fully glassy ribbons obtained by single roll melt-spinning [35].

The highest wear resistance after dry sliding wear test was demonstrated by the coatings obtained at 50 – 70% of the explosive charge. These coatings also showed high COF values in the range of 0.67 – 0.69. Similar values of wear resistance and COF of the coatings obtained at an explosive charge of 50 – 70% can be associated with close values of porosity, hardness and crystalline phase content of the coatings. The average wear resistance value of $Fe_{66}Cr_{10}Nb_5B_{19}$ detonation coatings obtained at an explosive charge of 50 – 70% was 6.7 ± 0.6 (10^{13} Pa).

The reduction of wear resistance of the coatings obtained at 40% of the explosive charge can be explained by low cohesion between the splats. As shown in our previous study [25], using 40% of the explosive charge, only particles with a size of 45 μm achieved temperatures to the molten state of the $Fe_{66}Cr_{10}Nb_5B_{19}$ alloy. The remaining particles in the 45 – 75 μm fraction did not remained solid or semi-solid upon the spraying process. Therefore, the coating was formed by molten particles of 45 μm size, and heated deformed particles of larger size.

Figure 3 presents images of the worn surface after a dry linearly reciprocating test of the coating obtained at 60% of the explosive charge. The worn surface exhibited deep scratches, grooves and particle delamination along the sliding direction (showed by arrows in Fig. 3 a), indicative of an abrasive wear mechanism. Particle delamination can be associated with a low temperature in the contact zone of the counterpart and coating, which is below the glass transition temperature (T_g) in a condition where the glass behaves as a solid with high viscosity. Particle delamination indicates a fatigue wear mechanism. The delaminated particles stayed in the worn surface and served as abrasive particles. However, the wear resistance of stainless steel was several times lower compared to the $Fe_{66}Cr_{10}Nb_5B_{19}$ detonation sprayed coatings. The results of the elemental analysis of the worn surface indicate a transfer of the counterpart material to the coating surface (Fig. 3 c). It is connected with a partial destruction of the counterpart.

3.2. Results of the nanohardness measurements, Young's modulus calculation and scratch tests of coatings

The volume loss of $Fe_{66}Cr_{10}Nb_5B_{19}$ detonation coatings after nanoscratch tests and nanohardness are presented in Table 1.

Table 1. The hardness, average COF value in the steady-state stage, calculated wear resistance (R_w) after dry sliding tests, volume loss after scratch tests, and nanohardness of the $Fe_{66}Cr_{10}Nb_5B_{19}$ detonation coatings and stainless steel. All parameters the confidence intervals are given (for a confidence level of 0.95), except for average COF.

Material	Hardness, HV_{300}	Average COF value in the steady-state stage	Wear resistance, 10^{13} Pa	Volume loss after scratch test, μm³	Nanohardness, GPa
$Fe_{66}Cr_{10}Nb_5B_{19}$, 40%	770 ± 90	0.64	1.55 ± 0.15	220 ± 90	13.5 ± 2.0
$Fe_{66}Cr_{10}Nb_5B_{19}$, 50%	870 ± 165	0.69	6.55 ± 1.05	145 ± 30	14.0 ± 2.0
$Fe_{66}Cr_{10}Nb_5B_{19}$, 60%	855 ± 55	0.67	5.70 ± 0.30	155 ± 50	12.5 ± 2.5
$Fe_{66}Cr_{10}Nb_5B_{19}$, 70%	840 ± 80	0.69	7.80 ± 0.55	150 ± 25	15.0 ± 3.0
Stainless Steel	≈220	0.58	0.70 ± 0.05	–	–

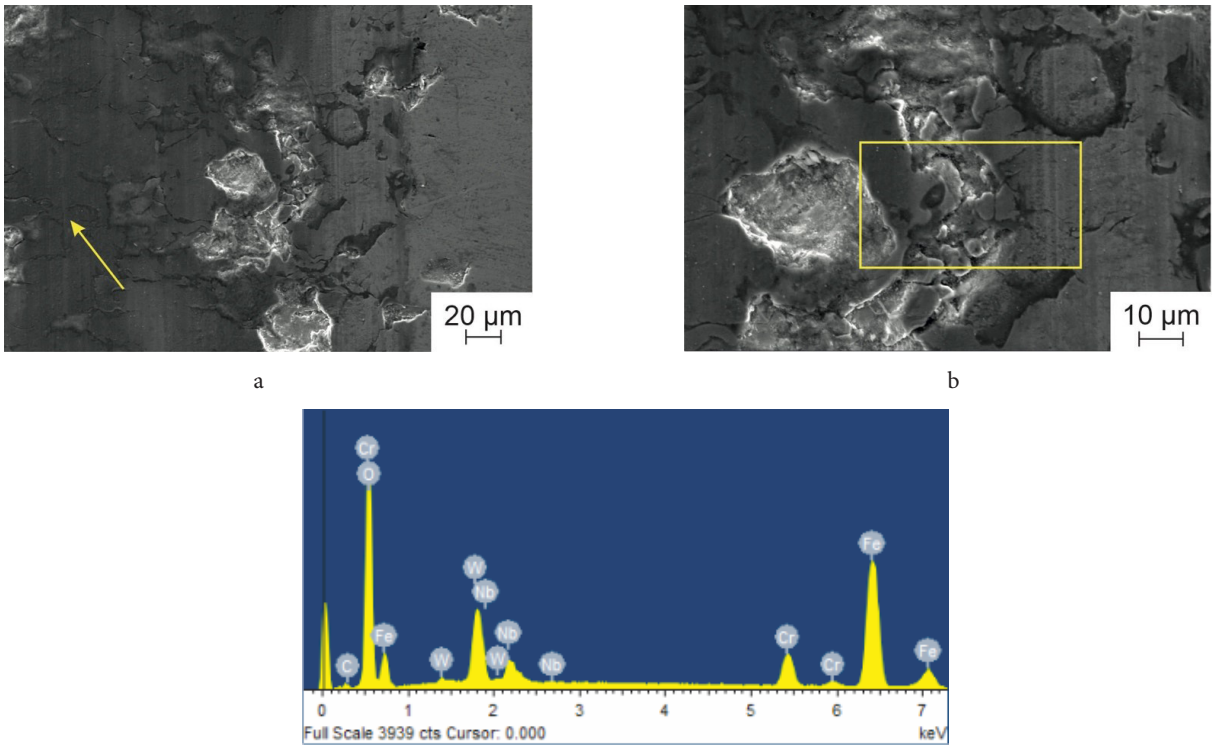

Fig. 3. SEM micrographs of the worn surfaces of the $Fe_{66}Cr_{10}Nb_5B_{19}$ glassy coating obtained at 60% of the explosive charge: low-magnification (a), high-magnification (b), results of the elemental analysis of the worn surface of the area selected in Fig. 3b (c). Deep scratches were shown by the arrow.

This series of coatings shows close values (considering the given values of confidence intervals) of wear resistance (average volume loss value 170 ± 50 μm^3) and nanohardness (average value 14 ± 2 GPa).

The structure of the detonation coatings presented in this work exhibits pores, microcracks and crystalline phases in the intersplat [25]. The increase in the scratch depth of the coating obtained using 40% of an explosive gas mixture ($O_2/C_2H_2 \approx 1$) was a result of the heterogeneous structure like the presence of pores. Due to the brittle nature of amorphous alloys and high stresses on the walls of pores and microcracks during the diamond tip indentation into the surface of the coatings the cracks propagation started. When the tip was moving during the scratch test the cracks was grown on the coating surface. The scratch depth (in length) of these coatings is significantly less (450 – 600 nm) compared to the coating obtained at an explosive charge of 40% (2 μm). The penetration depth depends on hardness and Young's modulus of materials. According to the standardized Oliver and Pharr method the Young's modulus of the coatings were calculated [36]. The Young's modulus of the detonation coatings obtained at 40%, 50%, 60%, and 70% of the explosive charge were 140 ± 25, 160 ± 30, 195 ± 30, and 215 ± 25 GPa, respectively. It can be seen that with increasing volume of explosive mixture the modulus of elasticity rises, which is associated with a reduction in the defects of the coatings and agrees with other publications [16, 37].

Y. Wu et al. [38] investigated the wear behavior under nanoscratch tests of SAM2X5 and SAM1651 coatings sprayed by high-velocity air fuel technology. The wear resistance of the obtained coatings was four times higher than that of the stainless steel. It was shown that porosity had a significant effect on the wear resistance of coatings. It should be noted that the nanohardness, Young's modulus and wear resistance of the $Fe_{66}Cr_{10}Nb_5B_{19}$ glass coatings are higher compared to the coatings presented in [38]. The nanoscratch resistance correlates strongly with nanohardness. The wear resistance under nanoscratch tests of the $Fe_{66}Cr_{10}Nb_5B_{19}$ coatings obtained in wide range of detonation modes does obey the J. F. Archard modified wear equation.

4. Conclusions

Wear resistant $Fe_{66}Cr_{10}Nb_5B_{19}$ coatings have been obtained in a wide range of detonation spraying modes. The wear behavior of detonation coatings under dry linearly reciprocating conditions and nanoscratch tests under ramping loads was investigated. The wear resistance under dry linearly reciprocating conditions of the obtained coatings are near nine times higher than that of stainless steel. The main wear mechanisms of detonation coatings under dry linearly reciprocating sliding conditions were fatigue and abrasive. The values of volume loss (after nanoscratch testing) and nanohardness are similar for the detonation coatings presented in this work. The scratch and spalling mechanisms of ploughing occurred due to the crack initiation and propagation from the walls of pores.

Acknowledgements. This study was performed within the framework of the State Contract of Lavrentyev Institute of Hydrodynamics of SB RAS (State Registration Number FWGG-2019-0003). The research was conducted at the core

facility "Structure, mechanical and physical properties of materials". The study was conducted at the Equipment Sharing Center "Mechanics" of ITAM SB RAS.

References

1. A. Inoue, A. Takeuchi. Acta Mater. 59 (6), 2243 (2011). Crossref
2. C. Suryanarayana, A. Inoue. Int. Mater. Rev. 58 (3), 131 (2013). Crossref
3. H. Fujimori, T. Masumoto, Y. Obi, M. Kikuchi. Japanese Journal of Applied Physics. 13 (11), 1889 (1974). Crossref
4. K. Miyoshi, D.H. Buckley. Wear. 110 (3), 295 (1986). Crossref
5. S. Pang, T. Zhang, K. Asami, A. Inoue. Acta Mater. 50 (3), 489 (2002). Crossref
6. Z.P. Lu, C.T. Liu, J.R. Thompson, W.D. Porter. Phys. Rev. Lett. 92 (24), 245503 (2004). Crossref
7. E.D. Zanotto, J.C. Mauro. J. Non. Cryst. Solids. 471, 490 (2017). Crossref
8. H.R. Ma, J.W. Li, J. Jiao, C.T. Chang, G. Wang, J. Shen, X.M. Wang. Mater. Sci. 33 (1), 65 (2016). Crossref
9. J.E. Berger, R. Schulz, S. Savoie, J. Gallego, C.S. Kiminami, C. Bolfarini, W.J. Botta. Surf. Coat. Technol. 309, 911 (2017). Crossref
10. G.Y. Koga, T. Ferreira, Y. Guo, D.D. Coimbrão, A.M. Jorge Jr., C.S. Kiminami, C. Bolfarin, W.J. Botta. J. Non. Cryst. Solids. 555, 120537 (2021). Crossref
11. W. Wang, C. Zhang, Z.-W. Zhang, Y.-C. Li, M. Yasir, H.-T. Wang, L. Liu. Sci. Rep. 7 (1), 4084 (2017). Crossref
12. T. Terajima, F. Takeuchi, K. Nakata, S. Adachi, K. Nakashima, T. Igarashi. J. Alloys Compd. 504, 288 (2010). Crossref
13. S. Yoon, J. Kim, B.D. Kim, C. Lee. Surf. Coat. Technol. 205 (7), 1962 (2010). Crossref
14. B. Fu, D. He, L. Zhao. J. Alloys Compd. 480 (2), 422 (2009). Crossref
15. Y. Qin, Y.P. Wu, Y. Zheng, Sh. Hong, J. Guo. Transactions of The China Welding Institute. 35, 103 (2014).
16. A.M. Hodge, T.G. Nieh. Intermetallics. 12, 741 (2004). Crossref
17. I.D. Kuchumova, I.S. Batraev, N.Y. Cherkasova, D.K. Rybin, A.V. Ukhina, W.J. Botta, G.Y. Koga, A.M. Jorge Jr. Mater. Today: Proc. 25 (3), 384 (2020). Crossref
18. J.A. Gan, C.C. Berndt. J. Therm. Spray Technol. 22 (7), 1069 (2013). Crossref
19. F. Tang, L. Ajdelsztajn, G.E. Kim, V. Provenzano, J.M. Schoenung. Surf. Coat. Technol. 185 (2–3), 228 (2004). Crossref
20. C.-J. Li, W.-Y. Li. Surf. Coat. Technol. 162 (1), 31 (2003). Crossref
21. H. Zhang, S. Wang, H. Li, S. Wang, Y. Chen. Coatings. 12, 176 (2022). Crossref
22. J. Kim, K. Kang, S. Yoon, S. Kumar, H. Na, C. Lee. Acta Mater. 58 (3), 952 (2010). Crossref
23. L. Xie, Y.-M. Wang, X. Xiong, Z.-K. Chen Mater. Trans. 59 (10), 1591 (2018). Crossref
24. H. Wu, X. Lan, Y. Liu, F. Li, W. Zhang, Z. Chen, X. Zai, H. Zeng. Trans. Nonferrous Met. Soc. China. 26 (6), 1629 (2016). Crossref
25. I.D. Kuchumova, I.S. Batraev, V.Yu. Ulianitsky, A.A. Shtertser, K.B. Gerasimov, A.V. Ukhina, N.V. Bulina, I.A. Bataev, G.Y. Koga, Y. Guo, W.J. Botta, H. Kato, T. Wada, B.B. Bokhonov, D.V. Dudina, A.M. Jorge Jr. Metals. 9 (8), 846 (2019). Crossref
26. K. Yoshida, M. Bito, J. Kageyama, Y. Shimizu, M. Abe, A. Makino. AIP Advances. 6 (5), 055933 (2016). Crossref
27. C.R.M. Afonso, C. Bolfarini, W.J. Botta, C.S. Kiminami. Mater. Sci. Forum. 727, 468 (2012). Crossref
28. J.C. Farmer, J.J. Haslam, S.D. Day. ECS Transactions. 3 (31), 485 (2007). Crossref
29. I.D. Kuchumova, I.S. Batraev, N.Y. Cherkasova, A.V. Ukhina, A.A. Shtertser, A.M. Jorge Jr. Metal Working and Material Science. 22 (3), 95 (2020). (in Russian) Crossref
30. I.D. Kuchumova, M.A. Eryomina, N.V. Lyalina, D.V. Dudina, I.S. Batraev, V.Y. Ulianitsky, A.A. Shtertser, N.Yu. Cherkasova, A.A. Ruktuev, A.V. Ukhina, T.A. Borisenko, G.Yu. Koga, C.S. Kiminami, A.M. Jorge Jr. J. Mater. Eng. Perform. 31, 622 (2022). Crossref
31. V.E. Gromov, Yu.F. Ivanov, O.A. Stolboushkina, S.V. Konovalov. Mater. Sci. Eng. 527 (3), 858 (2010). Crossref
32. D.V. Orlova, V.I. Danilov, L.B. Zuev, O.S. Staskevich. Physics of the Solid State. 58 (1), 9 (2016). Crossref
33. D.V. Orlova, V.I. Danilov, L.B. Zuev. Physics of the Solid State. 55 (2), 353 (2013). Crossref
34. A.L. Greer, K.L. Rutherford, I.M. Hutchings. Int. Mater. Rev. 47 (2), 87 (2002). Crossref
35. H.X. Li, Z.C. Lu, S.L. Wang, Y. Wu, Z.P. Lu. Prog. Mater. Sci. 103, 235 (2019). Crossref
36. W.C. Oliver, G.M. Pharr. J. Mater. Res. 7, 1564 (1992). Crossref
37. Y. Huang, Y.L. Chiu, J. Shen, Y. Sun, J.J.J. Chen. Intermetallics. 18 (5), 1056 (2010). Crossref
38. Y. Wu, Q. Luo, J. Jiao, X. Wei, J. Shen. Metals. 7 (4), 118 (2017). Crossref